Simulation of the EXAFS and Raman spectra of $In_xGa_{1-x}N$ utilizing the equation of motion routine of FEFF8.

2016 J. Phys.: Conf. Ser. 712 012126

(http://iopscience.iop.org/1742-6596/712/1/012126)

Journal of Physics: Conference Series **712** (2016) 012126 doi:10.1088/1742-6596/712/1/012126

Simulation of the EXAFS and Raman spectra of $In_xGa_{1-x}N$ utilizing the equation of motion routine of FEFF8.

M Katsikini[1*], F Pinakidou[1], E C Paloura[1], J Arvanitidis[1], S Ves[1], U Reinholz[2], E Papadomanolaki[3] and E Iliopoulos[3]

[1] Aristotle University of Thessaloniki, School of Physics, 54124 Thessaloniki, Greece
[2] BAM Federal Institute for Materials Research and Testing, 12200 Berlin, Germany
[3] University of Crete, Department of Physics and IESL-FORTH, 70013 Heraklion-Crete, Greece

* E-mail: katsiki@auth.gr

Abstract. A combined analysis of EXAFS and Raman spectra is applied for the study of $In_xGa_{1-x}N$ alloys with $0.3<x<0.5$. Alloying causes relaxation of the selection rules resulting in Raman spectra that resemble the vibrational density of states. On the other hand, theoretical simulation of the Raman spectra using the Equation of Motion routine of FEFF8 provides the vibrational component of the Debye-Waller factor (DWF). The static disorder component of the DWFs was obtained by fitting the Ga and In *K*-edge EXAFS spectra. The analysis revealed that the nearest neighbor distances of the 1st and 2nd shell deviate from the values predicted by the law of Vegard and the virtual crystal approximation. The static disorder in the first nearest neighboring shell (In-N and Ga-N) is null whereas in the cation-cation neighboring shells the static component is generally smaller than the vibrational.

1. Introduction

The tunability of the direct band gap of $In_xGa_{1-x}N$ alloys from near-IR to UV, by varying x, renders them important materials for photonic and optoelectronic applications as well as for efficient solar energy conversion devices [1,2]. InN, GaN and their alloys crystallize in the wurtzite structure where a cation (Ga, In) and a N *hcp* sublattice interpenetrate so as both the N and the cations are tetrahedrally coordinated. Although the lattice constants determined by X-ray diffraction (XRD) obey the law of Vegard, it has been theoretically predicted [3,4] and experimentally verified [5-8] that the In-N and Ga-N bonds retain their length close to the corresponding values in the binary compounds. As a result, the virtual crystal approximation (VCA), which assumes that all atoms occupy the average lattice positions defined by the lattice constants as determined by XRD [9], breaks down since the In and Ga atoms are displaced from their ideal positions and three different second nearest neighbor (*nn*) distances are detected in the cation sublattice (i.e. In-In, Ga-Ga, In-Ga) [10]. These local distortions affect the periodic lattice potential and consequently the carrier mobility [11]. Local fluctuations in the periodic potential reduce strongly the mean phonon free path, causing relaxation of the selection rules in the Raman spectra which become proportional to the vibrational density of states (VDOS) [12,13]. Extended X-ray absorption fine structure (EXAFS) spectroscopy is well suited for the study of local variations in the bonding geometry of the absorbing atom (for example In and Ga). The ratio of In/Ga atoms that populate the second *nn* shell is also obtained along with information on the static and thermal disorder described by the Debye-Waller factor (DWF). Assuming harmonic thermal vibrations

and symmetric atom pair distribution functions [14], the latter can be written as a sum of a vibrational and a static component i.e. $\sigma^2 = \sigma^2_{vib} + \sigma^2_{stat.}$ In this work, we benefit from the equation of motion routine [15,16] of the FEFF8 program [17] in order to simulate the Raman spectra of $In_xGa_{1-x}N$ alloys with $0.3<x<0.5$ and to obtain the σ^2_{vib}. The σ^2_{stat} component is determined from the analysis of the Ga and In *K*-edge EXAFS spectra of the same samples.

2. Growth conditions and experimental details

The $In_xGa_{1-x}N$ layers with x values 0.32, 0.37, 0.42 and 0.48 were grown by plasma-assisted molecular beam epitaxy on Al_2O_3 (0001) substrates using AlN buffer layers. The In/Ga flux ratio was kept the same for all the samples whereas the growth temperature was varied, from 520 to 400 ^oC, in order to control the In content [18]. The *a* and *c* lattice constants were determined from XRD measurements. The Ga and In *K*-edge EXAFS spectra were recorded in the fluorescence yield mode, at room temperature at the KMC-II and BAM*line* beamlines, respectively, of the BESSY II storage ring at the Helmholtz Zentrum, Berlin. The Raman spectra were recorded in the backscattering geometry using a micro-Raman system and the 457.9 nm line of an Ar+ laser for the excitation.

3. Results and discussion

A representative Raman spectrum of the sample $In_{0.48}Ga_{0.52}N$ is shown in figure 1. Strong enhancement in the intensity around the longitudinal optical (LO) modes is observed due to resonance effects as the energy gap of the studied samples approaches the energy of the laser line. The lattice constants were used for the construction of a cluster of approximately 200 atoms taking into account the In/Ga ratio. The force constants, k, listed in table 1 for the cation-cation, cation-N and N-N atom pairs were used for the simulation of the Raman spectra as shown in figure 1. The contribution in the VDOS of various scattering paths is also shown in figure 1. As expected, cation-N and cation-cation shells contribute in the high- and low-frequency part of the spectrum, due to the small and large reduced mass of the atom pair, respectively. The σ^2_{vib} values listed in table 1 were determined after fitting the projected VDOS for each path [15,16].

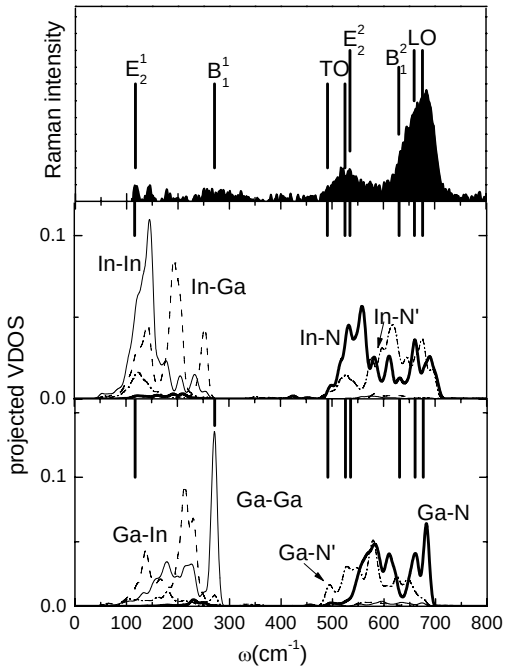

Figure 1. *Top:* Raman spectrum of the $In_{0.48}Ga_{52}N$ sample; *Middle:* Calculated VDOS, using the equation of motion routine, projected in the first (In-N), second (In-In and In-Ga) and third (In-N´) *nn* shells of In; *Bottom:* Calculated VDOS projected in the first (Ga-N), second (Ga-Ga and Ga-In) and third (Ga-N´) *nn* shells of Ga; Vertical lines denote the Raman frequencies of the vibrational transverse optical (TO), longitudinal optical (LO) and E_1, E_2 and B_1 modes of $In_{0.5}Ga_{0.5}N$.

Table 1. Atom-pair force constants, k, used for the calculation of the projected VDOS and σ^2_{vib}, obtained using the equation of motion method for the paths G1-G6 (Ga-N, Ga-Ga, Ga-In, Ga-N´, Ga-Ga-N and Ga-In-N, respectively) and I1-I6 (In-N, In-In, In-Ga, In-N´, In-In-N and In-Ga-N, respectively). x=1 and 0 correspond to InN and GaN binary compounds.

	k (N/m)						**$\sigma^2_{vib}\times10^{-3}$ (Å^2)**											
x	**Ga-N**	**In-N**	**Ga-Ga**	**In-In**	**Ga-In**	**N-N**	**G1**	**G2**	**G3**	**G4**	**G5**	**G6**	**I1**	**I2**	**I3**	**I4**	**I5**	**I6**
1	-	100	-	27	-	20	-	-	-	-	-	-	3.9	5.4	-	8.3	4.0	-
0.48	135	112	23	8	12	32	3.5	5.3	6.4	8.1	3.9	4.2	3.5	6.9	6.9	8.3	4.5	4.9
0.42	130	118	25	15	18	35	3.2	5.1	7.1	7.5	3.6	5.0	3.2	5.2	5.0	6.9	3.8	3.9
0.37	132	120	28	20	17	35	3.2	4.7	4.9	7.1	4.0	3.9	3.2	5.2	5.1	6.8	3.9	3.8
0.32	135	125	30	20	25	35	3.6	4.5	4.9	6.7	3.6	3.5	3.4	5.0	4.7	6.9	3.5	3.6
0	135	-	40	-	-	30	3.0	4.1	-	6.0	3.0	-	-	-	-	-	-	-

The EXAFS spectra recorded at the Ga and In *K*-edges were fitted using scattering paths that were constructed using the experimentally determined lattice constants. The σ^2_{vib} component of the DWF was set equal to the values listed in table 1. The fitting was performed for the 1st (4 N atoms), 2nd [12·x In and 12·(1-x) Ga atoms] and 3rd (9 N atoms) *nn* shells. The triangular scattering cation-cation-N paths were also considered with their path-length fixed according to the *nn* distances of the 1st and 2nd shell. The σ^2_{stat} component of the DWF was set equal to the value of the corresponding cation-cation path since the cation-N path is characterized by null σ^2_{stat}. Fitting of the Ga and In *K*-edge spectra in the k- and R-space is shown in figure 2 and the fitting parameters are listed in table 2.

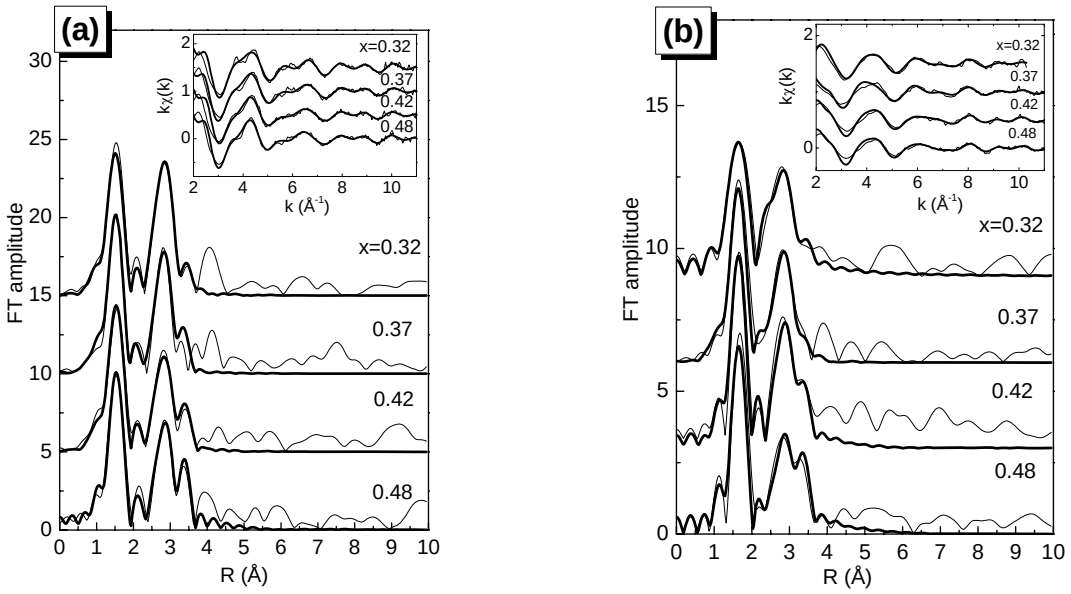

Figure 2. Fourier transform amplitude of the k^3-weighted χ(k) EXAFS spectra recorded at the (a) Ga and (b) In *K*-edge. The k^3-weighted χ(k) spectra are shown in the inset. The experimental and fitting curves are shown in thin and thick solid lines, respectively.

The results verify safely the violation of the VCA, as it is deduced from different Ga-N and In-N distances. Consequently, the local strain induced by alloying is mainly accommodated by cation–N–cation bond bending rather than cation–N bond stretching. Splitting is also observed in the 2nd *nn* shell. Regarding the DWF, the σ^2_{stat} contribution is null for the 1st *nn* shell. In the 2nd *nn* shell the values of σ^2_{stat} are generally smaller compared to the σ^2_{vib}.

Table 2. Fitting results of the In and Ga *K*-edge EXAFS spectra of the $In_xGa_{1-x}N$ samples for the 1st (cation-N) and 2nd (cation-cation) *nn* shells. x_{XRD} and x_{EXAFS} is the In molar fraction determined by XRD and EXAFS, respectively, R (Å) is the *nn* distance and $\sigma^2_{stat} \times 10^{-3}$ (Å^2) is the static component of the DWF.

		In-N		Ga-N		In-In		Ga-Ga		In-Ga	
x_{XRD}	x_{EXAFS} ±15%	R± 0.01	σ^2_{stat}	R± 0.01	σ^2_{stat}	R± 0.02	σ^2_{stat}± 30%	R± 0.02	σ^2_{stat}± 30%	R± 0.02	σ^2_{stat} ± 30%
0.48	0.49	2.13	0.0	1.97	0.0	3.39	1.6	3.28	0.9	3.33	3.3
0.42	0.40	2.12	0.0	1.96	0.1	3.38	3.7	3.27	2.6	3.33	2.8
0.37	0.36	2.13	0.0	1.95	0.0	3.36	5.2	3.24	2.8	3.30	5.5
0.32	0.33	2.12	0.2	1.96	0.0	3.36	2.9	3.24	1.9	3.29	5.2

4. Conclusions

The vibrational and static disorder component of the DWF of the Ga and In *K*-edge EXAFS spectra of $In_xGa_{1-x}N$ were determined utilizing the equation of motion routine of the FEFF8 software and the VDOS obtained by means of Raman spectroscopy. The static disorder component is found null for the cation-N pairs whereas in the 2nd *nn* cation-cation shells the static disorder component was found generally smaller compared to the thermal component. Finally, splitting in the distances in the 1st and 2nd *nn* shell imposes that local distortions caused by alloying are accommodated mainly by bond bending

Acknowledgements

This work is supported by the European Union (European Social Fund – ESF) and Greek national funds through the Operational Program "Education and Lifelong Learning" of the National Strategic Reference Framework (NSRF)-Research Funding Program: THALES, project NitPhoto. The measurements at BESSY II were funded from the European Community's Seventh Framework Programme (FP7/2007-2013) under grant agreement no.312284.

References

[1] Kamiyama S, Amano H and Akasaki I 2005 The Evolution of Nitride Semiconductors *Optoelectronic Devices: III Nitrides* ed. M Razeghi and M Henini (Oxford: Elsevier) chapter 3 pp 23–38.
[2] McLaughlin D V P and Pearce J M 2013 *J Met. Mater. Trans.* **A44** 1947.
[3] Ferhat M and Bechstedt F 2002 *Phys. Rev.* **B44** 07523.
[4] Saito T and Arakawa Y 1999 *Phys. Rev.* **B60** 1701.
[5] O' Donnell K P *et al*. 2001 *J. Phys. Cond. Mat.* **13** 6977.
[6] Katsikini M *et al.* 2003 *Nucl. Instrum. Meth.* **B200**, 114.
[7] Kachkanov V, O'Donnel K P, Pereire S and Martin R W 2007 *Philos. Mag*. **87** 1999.
[8] Katsikini M *et al.* 2008 *Phys. Status Sol.* ***A*****205** 2593.
[9] Mikkelsen Jr. J C and Boyce J B 1982 *Phys. Rev. Lett.* **49** 1412.
[10] Waychunas G A, Dollase W A and Ross II C R 1994 *Am. Mineral.* **79** 274.
[11] Adachi A 1994 *GaAs and related materials* (Singapore: World Scientific Publishing) chapter 14 p 556.
[12] Hernández S *et al.* 2005 *J. Appl. Phys.* **98** 013511.
[13] Katsikini M *et al.* 2010 *Phys. Status Solidi* **C7** 76.
[14] Mattila T and Zunger A 1999 *Phys. Rev.* **B85** 160.
[15] Poiarkova A V and Rehr J J 1999 *Phys. Rev.* **B59** 948.
[16] Poiarkova A V 1999 *X-ray absorption fine structure Debye-Waller factors* PhD Thesis, University of Wasington.
[17] Ankudinov A L, Ravel B, Rehr J J and Conradson S D 1998 *Phys. Rev.* **B58** 7565.
[18] Iliopoulos E *et al.* 2006 *Phys. Stat. Sol.* **A203** 102.